Old Dominion University

ODU Digital Commons

Electrical & Computer Engineering Faculty Publications

Electrical & Computer Engineering

1-2021

Generation of Excited Species in a Streamer Discharge

Shirshak K. Dhali

Follow this and additional works at: https://digitalcommons.odu.edu/ece_fac_pubs

 Part of the Electrical and Computer Engineering Commons, Materials Science and Engineering Commons, Nanoscience and Nanotechnology Commons, and the Physics Commons

AIP Advances

Generation of excited species in a streamer discharge

Cite as: AIP Advances **11**, 015247 (2021); https://doi.org/10.1063/5.0033110
Submitted: 14 October 2020 . Accepted: 02 January 2021 . Published Online: 29 January 2021

Shirshak K. Dhali

COLLECTIONS

Paper published as part of the special topic on Chemical Physics, Energy, Fluids and Plasmas, Materials Science and Mathematical Physics

View Online Export Citation CrossMark

ARTICLES YOU MAY BE INTERESTED IN

Simulation of decelerating streamers in inhomogeneous atmosphere with implications for runaway electron generation
Journal of Applied Physics **129**, 063301 (2021); https://doi.org/10.1063/5.0037669

Features of the secondary runaway electron flow formed in an elongated, atmospheric pressure air gap
Physics of Plasmas **27**, 103505 (2020); https://doi.org/10.1063/5.0024785

Transitions between electron emission and gas breakdown mechanisms across length and pressure scales
Journal of Applied Physics **128**, 210903 (2020); https://doi.org/10.1063/5.0030220

AIP Publishing

© 2021 Author(s).

Generation of excited species in a streamer discharge

Cite as: AIP Advances 11, 015247 (2021); doi: 10.1063/5.0033110
Submitted: 14 October 2020 • Accepted: 2 January 2021 •
Published Online: 29 January 2021

View Online Export Citation CrossMark

Shirshak K. Dhali[a)]

AFFILIATIONS

Department of Electrical and Computer Engineering, Old Dominion University, Norfolk, Virginia 23529, USA

[a)]Author to whom correspondence should be addressed: sdhali@odu.edu

ABSTRACT

At or near atmospheric pressure, most transient discharges, particularly in molecular gases or gas mixture containing molecular gases, result in a space charge dominated transport called a streamer discharge. The excited species generation in such discharges forms the basis for plasma chemistry in most technological applications. In this paper, we simulate the propagation of streamers in atmospheric pressure N_2 to understand the energy partitioning in the formation of various excited species and compare the results to a uniform Townsend discharge. The model is fully two-dimensional with azimuthal symmetry. The results show a significantly larger fraction of the energy goes into vibrational excitation of the N_2 ground state in a streamer-type discharge in comparison to a Townsend discharge. For lower applied voltages, the anode-directed (negative) steamer is slightly more efficient in channeling energy for excited species production in comparison to a cathode-directed (positive) streamer. Near 70% overvoltage, both types of streamers show very similar energy partitioning, but quite different from a Townsend discharge.

© *2021 Author(s). All article content, except where otherwise noted, is licensed under a Creative Commons Attribution (CC BY) license (http://creativecommons.org/licenses/by/4.0/).* https://doi.org/10.1063/5.0033110

I. INTRODUCTION

In most overvolted transient discharges at or near atmospheric pressure, an electron avalanche quickly leads to a space charge dominated transport called streamers. Streamers are precursors to arc and lightening formation. Since the streamer mechanism was first proposed by Raether[1] and Loeb and Meek,[2] a considerable amount of evidence has been accumulated, showing the importance of streamers or fast ionizing waves to the transient electrical breakdown of gases. The formation and propagation of streamers have been studied extensively both numerically[3–12] and experimentally.[13–16] Streamer properties depend on the density and composition of the gas, the temporal and spatial shape of the applied voltage, and its polarity. There are challenges to numerical studies of the streamer formation and propagation: The problem is inherently two-dimensional as a one-dimensional model has limited validity, and the steep density gradients encountered in the streamer front can lead to numerical instabilities.[3]

A review by Nijdam *et al.* discusses recent developments in diagnostics and simulation of streamers. They discuss the advances in numerical modeling including the pros and cons of particle-in-cell (PIC) and fluid models.[5] Luque and Ebert reviewed the density models for streamer discharge simulation, detailing their physical foundation, their range of validity, and the most relevant algorithm employed in solving them.[7] Fluid models used for streamer simulations require the knowledge of transport coefficients and rate coefficients that depend on the reduced electric field E/N. There has been a steady growth in the availability of open source codes such as BOLSIG+ to obtain these parameters for various gases and gas mixtures.[11] These types of solvers provide steady-state solutions of the Boltzmann equation for electrons in a uniform electric field using the classical two-term expansion.[8] Gordillo-Vazquez solved the coupled electron Boltzmann equation and rate equations for electrons, neutral, and ions to obtain the vibrational distribution function of electronic states of nitrogen molecules.[12] Simek and Bonaventura used a similar approach to simulate the kinetics of excited states by modeling the time variation of a streamer-like electric field.[11]

Most of the experimental work on streamers is based on the optical emission from the discharge. Shutter and streak photographic techniques have been used to measure the leading edge of the swarm.[15] Spectroscopic techniques can shed light on the spatial and temporal distribution of excited species in streamer discharges. Simek discussed optical emission spectroscopic methods

© Author(s) 2021

based on the two-dimensional projection of cylindrically symmetric streamers to determine the radial distribution of excited species within a streamer channel. Laser induced florescence (LIF) is also a powerful tool to map spatial and temporal distribution of excited species and radicals in a streamer discharge.[16] Ono discussed additional techniques such as absorption and coherent anti-Stokes Raman scattering methods to study reactive species in a streamer discharge.[14]

During the generation of a cold plasma at atmospheric pressure in dielectric-barrier discharges (DBDs) or pulsed discharges including pulsed corona discharges, the streamer phase is quenched prior to the formation of an arc by several mechanisms, such as dielectric charging and pulsing the voltage, or by the electrode geometry in corona discharges. Cold atmospheric-pressure plasmas are extensively used in many industrial applications such as treatment of polymer surfaces and textile fibers and abetment of toxic gases.[17–22] Weltmann *et al.* provided a detailed survey of the current status of plasma science and technology along with emerging applications.[21] The low pressure plasma in semiconductor industry is a prime example of a success story; however, many applications rely on atmospheric pressure non-thermal plasmas, such as plasma medicine.[18] Most of these applications are energy intensive as it relies on the production of free radicals in the electrical discharge to carry out the required plasma–chemical reactions.[19]

Although there are many reports of the analytical and computation study of streamer formation and propagation, however, there is limited information on how effective the streamers are in producing relevant radicals in the electrical discharge or the energy partitioning to the various inelastic energy loss pathways. There have been several reported-research studies on gas-phase remediation of toxic gases where the investigators estimated the yield of certain products. Penetrante reported on the plasma chemistry and power consumption in non-thermal plasma DeNO$_x$, which is compared to an electron beam process.[20] Marode *et al.* discussed high pressure discharges for pollution control and provided a comparison of streamer type discharge to a corona discharge.[22] These reports are limited to investigating radical production in uniform electrical discharges followed by relatively slow zero-dimension neutral chemistry. At atmospheric pressures, due to significant space charge, the excited species generation varies both temporally and spatially during the streamer propagation and assuming a zero-dimensional model for the discharge would lead to incorrect estimation of radical generation due to spatially varying electron temperature.

Boeuf and Kunhardt reported on the energy balance in a nonequilibrium weakly ionized discharge in nitrogen gas.[23] They studied the temporal development of the energy balance in a nitrogen discharge during its early phases by simulating the self-consistent calculation of the electron distribution function, the vibrational population, and densities of some electronically excited states. The emphasis was more on the interaction of these excited species and its effect on the electron distribution function. These calculations were done for uniform field and zero-dimension without considering the spatial and temporal variation of the electric field due to the space charge.

Our approach is to model the formation and propagation of the streamer phase of the discharge in atmospheric pressure N_2 and use the relevant streamer properties, such as spatial and temporal distribution of the electron density and reduced electric field, to calculate the production of electron impact generation of excited species. This information is used to calculate the energy partitioning into different channels as a function of time. We do this for both the anode-directed and cathode-directed streamers and compare these results to a uniform Townsend discharge. The goal of this work is not so much to provide quantitative numbers for energy partitioning, but to provide a qualitative understanding based on the streamer properties.

II. THE MODEL AND NUMERICAL METHODS

The electrical power in a discharge is primarily absorbed by the electrons and channeled to various electron impact processes, which is determined by the gas composition and the electron energy. The electrons lose energy through either elastic or inelastic collisions. The inelastic collisions such as electronic exaction, ionization, dissociation, and vibrational excitation in molecular gases dominate the energy loss. At or near atmospheric pressure, the neutral excited species play an important role in the subsequent plasma chemistry or photon emission. However, to better capture the quantitative analysis of the plasma chemistry, it is critical to understand how the energy is channeled to the numerous electron impact processes during the energy deposition phase.

The simplest fluid model to describe the steamer formation and propagation in the N_2 gas consists of the continuity equation for the electrons and positive ions coupled with Poisson's equation for the electric field along with various field dependent transport parameters and ionization coefficient,[3]

$$\frac{\partial n_e}{\partial t} + \vec{\nabla}.(\vec{v}_e n_e) - D_e \nabla^2 n_e = \alpha n_e v_e + S, \tag{1a}$$

$$\frac{\partial n_p}{\partial t} + \vec{\nabla}.(\vec{v}_p n_p) - D_p \nabla^2 n_p = \alpha n_e v_e + S, \tag{1b}$$

$$\nabla^2 \emptyset = -q_e(n_p - n_e)/\varepsilon_o, \tag{2}$$

where n_e, $\vec{v}_e$, D_e, n_p, $\vec{v}_p$, and D_p are the particle density, drift velocity, and diffusive for the electrons and positive ions, respectively, $v_e = |\vec{v}_e|$, and α is the Townsend ionization coefficient. The quantity S is various ion/electron source or sink mechanisms such as photoionization or recombination or remnant space charge in repetitive discharges. Photoionization is an important mechanism for streamer propagation in gas mixtures or gases containing impurities. However, in pure gases such as N_2, the self-photoionization in a discharge is not well understood. Since the photon energy greater than the ionization potential is required for photoionization, the ionizing radiation generated in electron impact processes leading to direct dissociative excitation (N I) or by direct ionizing excitation (N II) followed by a radiative transition of the excited neutral atom or ion is a possible pathway.[24] In an attaching gas, a third continuity equation for the negative ion species would be needed and the S term would be distinct for each species.

The electric field, E, is obtained from the potential, φ,

$$E = -\nabla \emptyset. \tag{3}$$

The set of Eqs. (1)-(3) is closed using the drift equations,

$$\vec{v}_e = -\mu_e E \text{ and } \vec{v}_p = \mu_p E.$$

© Author(s) 2021

The discharge current consists of displacement current given by

$$I_g = \frac{q_e}{d}\int_{gap}(\vec{v}_p n_p - \vec{v}_e n_e).\hat{e_z}d^3r, \quad (4)$$

where d is the gap distance and $\hat{e_z}$ is the unit vector in the z direction. The cumulative energy deposited in the gap, which is used to determine the energy partitioning, is given by

$$\varepsilon(t) = \int_0^t V_g(\tau)I_g(\tau)d\tau. \quad (5)$$

As stated earlier, the emphasis of this work is in understanding the production of excited species. A generic electron impact excitation process is shown in Eq. (6) where the rate coefficient $k_x(\hat{r}, t)$ is spatially and temporally dependent on the local reduced field (E/N) obtained from the streamer simulation. At each time step, Eq. (7) is used to calculate the generation of the excited species x from the spatial electron density distribution,

$$N_2 + e \xrightarrow{k_x} N_2^* + e, \quad (6)$$

$$N_x(t) = \int_0^t dN_x(t), \text{ where } dN_x(t) = \Delta t\int_{gap} n_e(\hat{r},t)k_x(\hat{r},t)d^3r, \quad (7)$$

with $N_x(t)$ being the total number of species x produced in the discharge. The fractional energy partition, FEP, as a cumulative function of time is obtained from the threshold energy (V_{xTH}) of the process and the cumulative discharge energy,

$$FEP = N_x(t) \times V_{xTH}/\varepsilon(t). \quad (8)$$

We used a polynomial fit to the experimental data[25] for the electron temperature as a function of the reduced electric field given by

$$T_e = 0.92 + 1.54 \times 10^{-2}(E/N) - 1.7 \times 10^{-5}(E/N)^2 + 7.8 \times 10^{-9}(E/N)^3, \quad (9)$$

where T_e is the electron temperature in Volt and E/N is the reduced electric field in Townsend (Td).

The rate coefficients of the electron impact with neutral molecules include elastic collisions, rotational excitation, vibrational excitation of the ground state, electronic excitation, and ionization. These rate coefficients can be obtained by solving the Boltzmann equation or Monte Carlo simulation starting from the cross sections. There are several reports available for rate coefficients for electron impact processes by the BOLSIG+ solver.[8,13] We have used for our simulations a set of rates calculated by Gudmundsson, assuming the electron energy distribution to be Maxwellian.[26] These rates are available as functions of the electron temperature. Although a Maxwellian distribution is assumed to calculate the rates, the compilation published by Gudmundsson is standalone and extensive and was the primary reason for using this in our calculations. These data were also fitted to an Arrhenius type of equation, which was easy to use. Since we are using the drift diffusion model, which assumes that the electrons rapidly relax to an equilibrium velocity distribution (not necessarily Maxwellian), the use of Maxwellian rate constants will not impact the qualitative results. However, if the PIC model was being used for the streamer simulation, then using rates derived from the kinetic model would be more appropriate.

In our approach, once the spatial and temporal distribution of electron density and the reduced field E/N is obtained from the streamer simulation, any excited species of interest can be studied if the rates are known as a function of E/N or electron temperature [Eq. (7)]. The other important transport coefficient is the electron drift, which is a function of E/N. Implicit in the electron drift are all channels of energy loss. The drift velocity along with electron density (and ion density) is enough to determine the current [Eq. (4)] and hence the power and energy deposited in the discharge.

To study the energy partitioning, we picked several representative electron impact processes. These include elastic collisions, several levels of the vibrational excitation of the ground state, and several triplet and singlet electronic states. In molecular gases, the vibrational energy, particularly of the ground state, is a significant source of inelastic energy loss. The $A^3\,\Sigma_u^+$ state was included since it is longed lived and impacts plasma processing, particularly in afterglows. The other triplet states included are significant in emission spectroscopic diagnostics of discharges. Although we did not explicitly look at N^2 dissociation, atomic nitrogen in a discharge is produced by the predissociation of an excited state. Both the singlet and triplet states at a high vibrational level will lead to dissociation into the atomic ground state, $N(^4S^0)$, or the excited states $N(^2D^0)$ or $N(^2P^0)$.[27] The $a'^1\Sigma_u$ state is known to dissociate in levels $v > 6$.[27] Therefore, this state was included in our study.

In nitrogen gas, for pressure (P) in Torr and electric field (E) in V/cm, the Townsend first ionization coefficient is

$$\alpha = 5.7e^{-260P/E}.$$

For the electric field of interest, the electron and positive ion mobilities are well approximated by a simple constant mobility model

$$\mu_e = 2.9 \times \frac{10^5}{P}\frac{\text{cm}^2}{Vs},$$

$$\mu_p = 2.6 \times \frac{10^3}{P}\frac{\text{cm}^2}{Vs}.$$

The transverse and longitudinal diffusion coefficients are $D_T = 1800\,\text{cm}^2/\text{s}$ and $D_L = 2190\,\text{cm}^2/\text{s}$, respectively.

The convective part of the continuity equation was solved with the two-dimensional flux-corrected techniques, which were developed by Boris and Book to model one-dimensional shock fronts in fluids.[28] It is well suited to handle the steep gradients that appear in front of the streamer head. The details of the two-dimensional method with azimuthal symmetry can be found in Ref. 3. Poisson's equation was solved using the implicit successive relaxation method (SOR). The SOR techniques are well suited for the streamer problem as there is only an incremental change in the space charge distribution at each time step and the convergence of the solution for the electric potential is relatively fast.[29]

© Author(s) 2021

III. RESULTS AND DISCUSSION

The simulation is done for a parallel plate geometry with a gap separation of d = 5 mm and N_2 at an atmospheric pressure of 760 Torr. For the numerical computation, we bypass the avalanche stage and start with an initial density, which quickly leads to the formation of the streamer stage. This is done by placing a Gaussian shaped semi-hemispherical initial charge of 0.5×10^{19} m^{-3} with a 1/e radii of 0.3 mm. To initiate only one type of streamer, either a cathode- or anode-directed streamer, the initial charge is placed on an electrode. We are primarily interested in reaching a steady streamer propagation from which the temporal and spatial electron density and electric field can be extracted to estimate the density of the excited species. In our simulation, the streamer formed after a short period (sub-ns) of adjustment and we could immediately numerically study the streamer propagation without having to go through the avalanche phase. Since the precise nature of photoionization is not well understood in pure nitrogen, for the calculations presented here, we have not included photoionization in the source term. Instead, as an initial condition, a tenuous neutral plasma of 10^{11} m^{-3} is included in the simulation for the "S" term in Eq. (1). The effect of these initial conditions on streamer characteristics has been reported in earlier publications.[3,4]

We did a set of simulations for both the anode- and cathode-directed streamers for applied voltages of 20 kV, 22 kV, 25 kV, and 30 kV across a 5 mm gap, and for a static breakdown voltage of 17.7 kV for such a gap in N_2, the applied voltages correspond to overvoltages of 16.4%, 24.3%, 41.2%, and 69.5%, respectively. A representative contour plot of the cross section through the axis at various times for an anode-directed streamer and a cathode-directed streamer for an applied voltage of 25 kV is shown in Fig. 1.

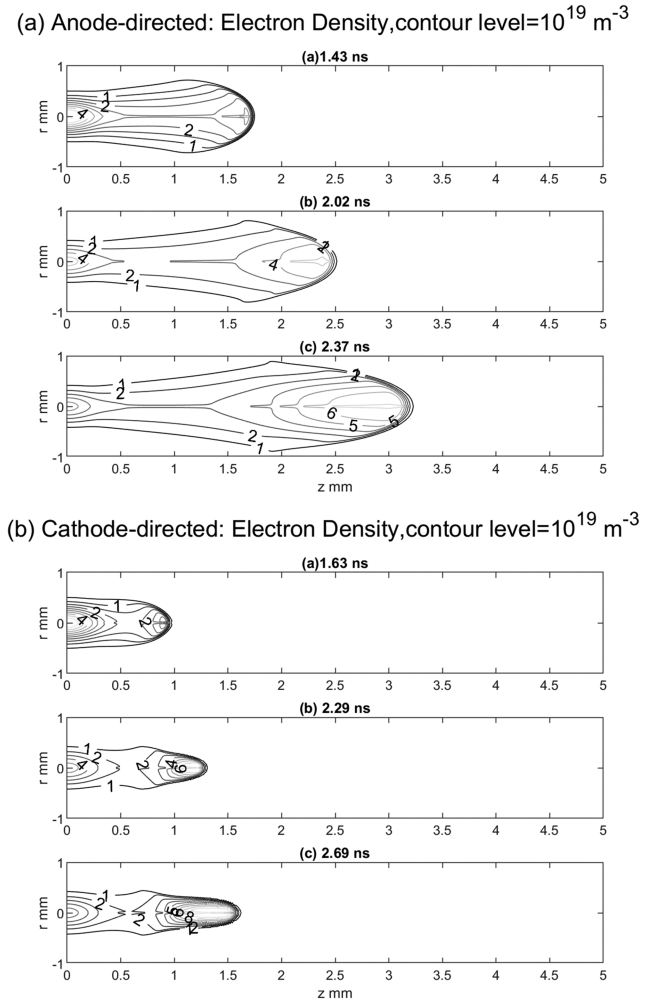

FIG. 1. Contour plot of the electron density for (a) an anode-directed streamer and (b) a cathode-directed streamer. The applied voltage to the 5 mm parallel-plate gap was 25 kV at a pressure of 760 Torr.

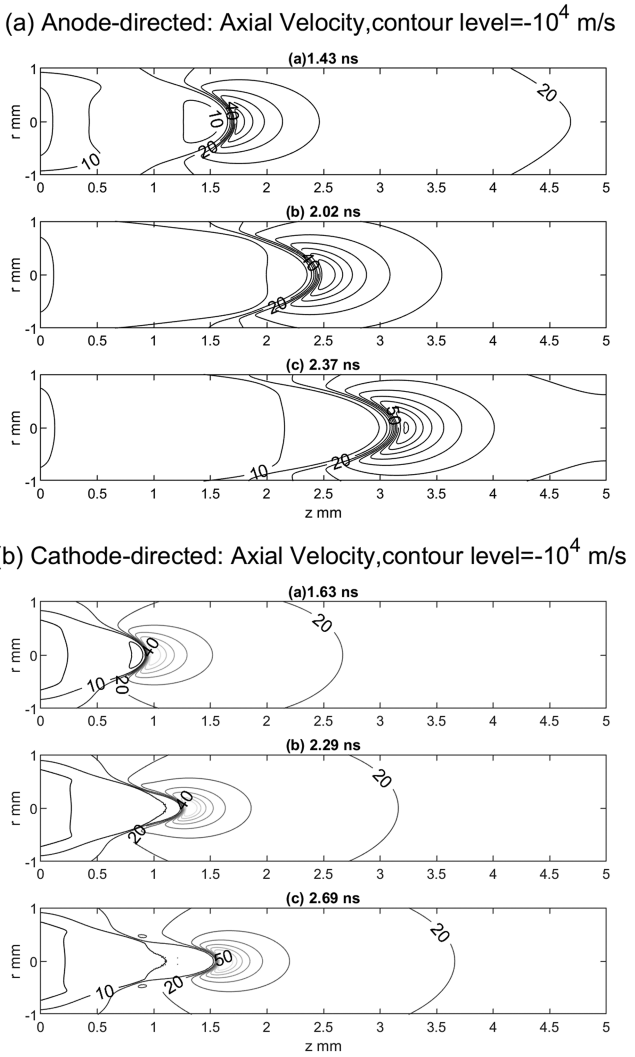

FIG. 2. Contour plot of the axial velocity of (a) an anode-directed streamer and (b) a cathode-directed streamer. The applied voltage to the 5 mm parallel-plate gap was 25 kV at a pressure of 760 Torr.

© Author(s) 2021

In our simulations, the streamer propagation starts after an initial adjustment phase of the neutral charge that was placed on the electrode. Once the streamer is fully formed, it attains the characteristic structure of a neutral plasma core with high space charge in the front of the streamer and reaches its mean propagation velocity. For a fully formed anode-directed streamer, the velocity of the ionization front is about 2.2×10^6 m/s and the diameter is about 1.5 mm. At a similar time into the simulation when the streamer is fully formed, the cathode-directed streamer front has a velocity of 0.87×10^6 m/s and a narrower diameter close to 1 mm. In an anode-directed streamer, the electron drift is in the same direction as the propagation of the streamer front, and for the cathode-directed streamer, it is in the opposite direction. As a comparison, the electron drift velocity at the externally applied field is 0.19×10^6 m/s. The difference in the propagation speed between the anode-directed streamer and the cathode-directed streamer is roughly twice the drift velocity at the applied field. Tarashenko *et al.* have reported the measurements of streamer velocity in air discharges and observed similar results with an anode-directed streamer propagation speed faster than the cathode-directed streamer.[30]

The spatial development of the axial velocity of the two streamer types at three different times is shown in Fig. 2. The spatial extent closely follows the density contour plot of Fig. 1. The field is shielded in the bulk of the streamer, and there is a considerable field enhancement at the tip. The shielding charge forms a thin shell of negative charge and positive charge for an anode-directed streamer and a cathode-directed streamer, respectively. The field ahead of the streamer tip drops rapidly to the applied field.

The discharge current is calculated at each time step according to Eq. (4) and is shown in Fig. 3 for an anode-directed streamer at an applied voltage of 25 kV across a 5 mm gap. Since a neutral charge is placed as an initial condition to simulate the formation of the streamer without going through the avalanche phase, the current shows an abrupt change at t = 0. Following an initial period of adjustment due to the finite dielectric relaxation time $\tau_D = \varepsilon_0/q_e\tilde{n}_e\mu_e$, the current starts to increase as the streamer channel starts to grow with time. Under the condition for the discharge parameters, $\tau_D \approx 0.03$ ns.

At each time step of the simulation, the spatial distribution of electron number density and the electric field is available. Using Eq. (7), the generation of the excited species can be calculated. This is integrated over time, and the energy partitioning is calculated, which is shown in Fig. 4 for the anode- and cathode-directed steamer. The following excited species number was calculated at each time step: $X^1\Sigma_g^+$ υ = 1–10, $A^3\Sigma_u^+$, $B^3\Pi_g$, $C^3\Pi_u$, $a'^1\Sigma_u^-$, and N_2^+. These excited species are important precursors to neutral–neutral chemistry. The metastable $A^3\Sigma_u^+$ plays an important role in afterglows with a lifetime in seconds.[31]

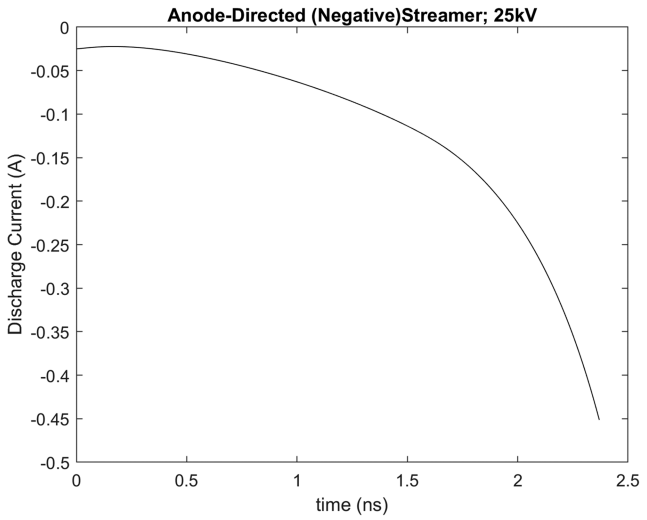

FIG. 3. The discharge current drawn for an anode-directed streamer with an applied voltage of 25 kV across a 5 mm gap filled with N_2 at 760 Torr.

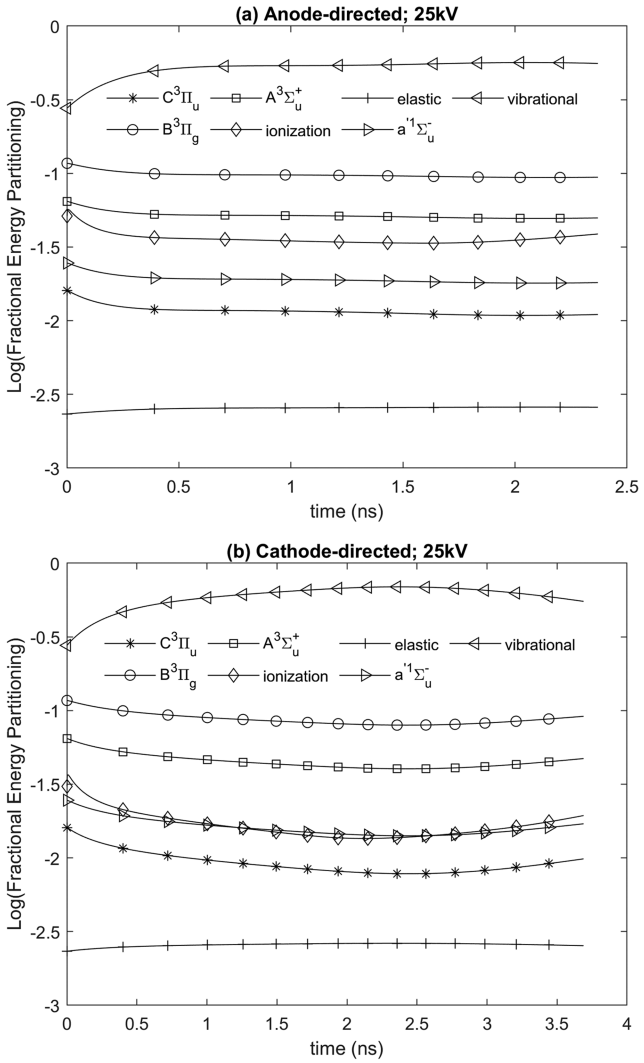

FIG. 4. The fractional energy partitioning for (a) an anode-directed streamer and (b) a cathode-directed streamer. The applied voltage was 25 kV to a 5 mm gap at a pressure of 760 Torr.

© Author(s) 2021

The anode-directed streamer energy-partitioning tends to reach a steady-state value after an initial adjustment. However, the cathode-directed steamer after a period of steady values shows changes. Since our simulation introduces a tenuous background of neutral free charge in place of photoionization, the buildup of this charge with time alters the propagation of the streamers beyond a time of 3 ns for the applied field in the case of 50 kV/cm.

Clearly, a significant fraction of the energy goes into the ground-state vibrational excitation, which is eventually lost to gas heating by the V–V or V–T exchange.[23] Due to the anharmonicity of the nitrogen molecule, the V–V reaction leads to gas heating. However, a non-negligible amount of energy lost in vibrational excitation can be recovered as electronic excitation in super-elastic collisions. The V–T exchange is particularly important at a higher vibrational quantum number.

The electron energy loss to elastic collision is low due to the large difference of masses between the electron and nitrogen molecule. Amongst the excited electronic states, the rates favor the formation $B^3\Pi_g$ for the electron energies in the streamer discharge, which gives rise to the emission of 600 nm–1200 nm attributed to the first-positive ($B^3\Pi_g \rightarrow A^3\Sigma_u^+$). The reduced electric field in the streamer discharges ranges from 100 to 1000 Td. This gives an electron energy range of 2.3 eV–7.5 eV calculated using Eq. (9). At a higher reduced electric field, the electron energy starts to saturate, and the increase is far from linear. Correspondingly, the electron temperature dependent rate coefficient tends to saturate, and the net effect of the high field enhancement is thus reduced.

The simulation was also run under conditions where the space charge was very low to create the conditions for a Townsend discharge. This is done by placing an initial neutral plasma ball of very low density (10^{11} m^{-3}). As expected, the fractional energy partitioning for a Townsend discharge did not change with time. This can also be deduced from the equation for current and excited species numbers shown in Eqs. (4) and (7), respectively. Since E/N is constant throughout the discharge volume due to the absence of space charge, the electron drift velocity and the rate coefficients are constants. The discharge current is primarily carried by the electrons due to its large mobility difference compared to ions. Therefore, both the current and excited species number are proportional to the total electrons in the discharge volume, and the ratio of the excited species number to energy in Eq. (8) is constant.

The results of the Townsend discharge were used as a baseline to compare the energy partitioning in the streamers. Figure 5 shows the comparison for a few (ground-state vibration, ionization, $B^3\Pi$, and $a'^1\Sigma_u$) selected species. A significantly large fraction of the input energy in streamer discharges goes into vibrational excitation compared to the Townsend discharge. Although there is considerable field enhancement at the streamer tip, in the bulk of the streamer channel, the electric field is lower than the applied field, which favors low threshold processes. This lowers the fractional energy partitioning in the high threshold process compared to a Townsend discharge. In addition, the rate coefficients start to flatten as E/N increases for all the processes we have included, thus diluting the effect of field enhancement in streamers. As a result of the high fraction of energy loss to vibrational excitation, the fraction of energy channeled to the excitation of the electronic states is considerably lower for the streamer discharges compared to the Townsend discharge.

The radial extent of a fully formed anode-directed steamer is larger compared to a cathode-directed streamer, as shown in

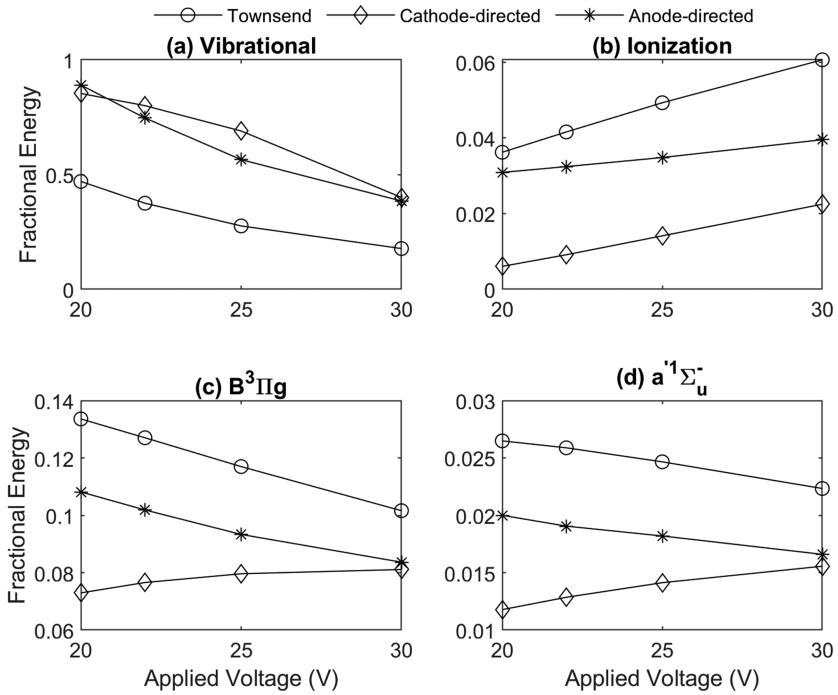

FIG. 5. Comparison of energy partitioning for four selected excitations: (a) Ground-state vibrational, (b) ionization, (c) triplet $B^3\Pi_g$, and (d) singlet $a'^1\Sigma^-_u$.

© Author(s) 2021

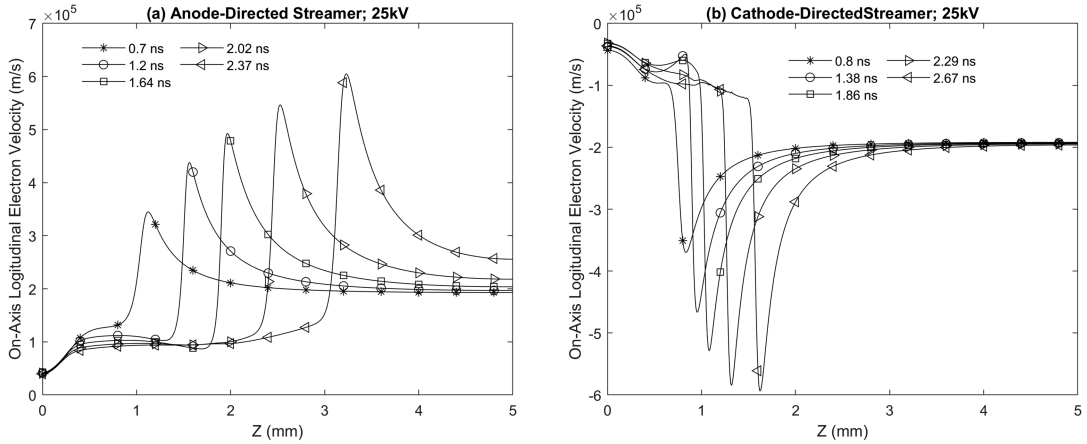

FIG. 6. (a) On-axis axial velocity for an anode-directed streamer at different times during the propagation. (b) On-axis axial velocity for a cathode-directed streamer at different times during the propagation. The applied voltage to the 5 mm parallel-plate gap was 25 kV at a pressure of 760 Torr.

the contour plots of Figs. 1 and 2. The extent to which the field enhancement extends beyond the tip of the streamer depends on the radii of the tip. In the extreme case of an infinite tip radius and complete shielding, the field enhancement can be a maximum of twice the value of the applied field, and it remains flat past the tip. As the radius decreases, the enhancement increases, but the spatial extension in front of the tip decreases. This is illustrated by the on-axis plot of the axial velocity for the anode- and cathode-directed streamers shown in Fig. 6. Therefore, in an anode-directed streamer, a greater number of electrons in front of the streamer front experience a larger field compared to the cathode-directed streamer. This field profile in an anode-directed streamer favors the formation of species with higher threshold energy. At higher overvoltages, the two streamers have similar properties in terms of electron density and field enhancement. This results in similar energy partitioning in both types of streamers for high applied fields.

There are reported results of species generated by streamers in atmospheric pressure plasma (APP) jets.[31] The work was primarily done for He plasma jets propagating outside of the core region where the plasma is produced. Our results differ from other reports as it focusses on how the energy partitioning is taking place as a function of time in the streamer as it is forming and propagating within the active region of the discharge. Clearly, it is advantageous to quench the discharge before a significant space charge build up. In many high-pressure APP jets, this is achieved by using fast rise-time short pulses limiting the space charge formation. In addition, narrow width dielectric barrier discharges would be more efficient in producing reactive species for plasma chemistry due to quick charging of the dielectric leading to quenching of the streamer.

As future work, we plan on studying the atomic gases and gas mixture containing attaching gases. In contrast to a molecular gas such as nitrogen in which a significant fraction of the energy goes into vibrational excitation, in atomic gases, most of the energy goes into electronic excitation and ionization. Since attaching gases form heavy negative ions, it is expected that the energy partitioning would be different in a gas such as oxygen, which is used in silent discharges for ozone generation.

IV. SUMMARY

We have studied in detail the formation and propagation of positive and negative steamers and compared the energy partitioning for the creation of various excited species to a uniform Townsend discharge at different applied voltages in a parallel plate gap. A fluid model and Maxwellian rate constants were used, which place some restriction on the region of validity but capture the relevant features at reduced complexity and computational cost. The vibrational energy partition in either streamer type is considerably higher than the uniform Townsend discharge. Since the vibrational energy eventually leads to gas heating, it reduces the efficiency of species creation in a streamer. Correspondingly, the energy channels for excitation are lower for streamer discharges in comparison to the Townsend discharge. The anode-directed (negative) streamer performs better in excited species creation compared to the cathode-directed (positive) streamer particularly at lower applied voltages. In applications, particularly at high pressures, where the efficiency of production of reactive radicals by the excited species is critical, a discharge should be limited or quenched prior to significant space charge accumulation such as short, pulsed discharges or narrow width dielectric-barrier discharges.

ACKNOWLEDGMENTS

This work was supported by the U.S. Department of Energy, Office of Fusion Energy Sciences Award No. DE-SC0020183.

DATA AVAILABILITY

The data that support the findings of this study are openly available in Refs. 25 and 26.

© Author(s) 2021

REFERENCES

[1] H. Raether, Z. Phys. **112**, 464 (1939); Arch. Electrotech. **34**, 49 (1940).
[2] L. B. Loeb and J. M. Meek, J. Appl. Phys. **11**, 438 (1940).
[3] S. K. Dhali and P. F. Williams, J. Appl. Phys. **62**, 4696 (1987).
[4] S. K. Dhali and A. K. Pal, J. Appl. Phys. **63**, 1355 (1987).
[5] S. Nijdam, J. Teunissen, and U. Ebert, Plasma Sources Sci. Technol. **29**, 103001 (2020).
[6] R. Morrow, Phys. Rev. A **32**, 1799 (1985).
[7] A. Luque and U. Ebert, J. Comput. Phys. **231**, 904 (2012).
[8] G. J. M. Hagelaar and L. C. Pitchford, Plasma Sources Sci. Technol. **14**, 722 (2005).
[9] A. Kulikovsky, J. Phys. D: Appl. Phys. **30**, 441 (1997).
[10] R. Dorai and M. J. Kushner, J. Phys. D: Appl. Phys. **36**, 666 (2003).
[11] M. Simek and Z. Bonaventura, J. Phys. D: Appl. Phys. **51**, 504004 (2018).
[12] F. J. Gordillo-Vazquez, J. Geophys. Res. **115**, A00E25, https://doi.org/10.1029/2009ja014688 (2010).
[13] M. Simek, J. Phys. D: Appl. Phys. **47**, 463001 (2014).
[14] R. Ono, J. Phys. D: Appl. Phys. **49**, 083001 (2016).
[15] W. J. Yi and P. F. Williams, J. Phys. D: Appl. Phys. **35**, 205 (2002).
[16] M. Simek, P. F. Ambrico, and V. Prukner, J. Phys. D: Appl. Phys. **48**, 265202 (2015).
[17] U. Kogelschatz, Plasma Chem. Plasma Process. **23**, 1 (2003).
[18] M. Laroussi, X. Lu, and M. Keidar, J. Appl. Phys. **122**, 020901 (2017).
[19] K. H. Becker, U. Kogelschatz, K. H. Schoenbach, and R. J. Barker, *Non-Equilibrium Air Plasmas at Atmospheric Pressure* (Institute of Physics Publishing, Bristol, 2005).
[20] B. M. Penetrante, in *Non-Thermal Plasma Techniques for Pollution Control, Part A: Overview, Fundamentals and Supporting Technologies*, NATO ASI Series, edited by B. M. Penetrante and S. E. Schultheis (Springer-Verlag, 1993), p. 65.
[21] K. D. Weltmann, J. F. Kolb, M. Holub, D. Uhrlandt, M. Simek, K. Ostrikov, S. Hamaguchi, U. Cvelbar, M. Cernak, B. Locke, A. Fridman, P. Favia, and K. Becker, Plasma Processes Polym. **16**, e1800118 (2019).
[22] E. Marode, A. Goldman, and M. Goldman, in *Non-Thermal Plasma Techniques for Pollution Control, Part A: Overview, Fundamentals and Supporting Technologies*, NATO ASI Series, edited by B. M. Penetrante and S. E. Schultheis (Springer-Verlag, 1993), p. 167.
[23] J. P. Boeuf and E. E. Kunhardt, J. Appl. Phys. **60**, 915 (1986).
[24] S. Pancheshnyi, Plasma Sources Sci. Technol. **24**, 015023 (2015).
[25] L. Campbell, M. J. Brunger, A. M. Nolan, L. J. Kelly, A. B. Wedding, J. Harrison, P. J. O. Teubner, D. C. Cartwright, and B. McLaughlin, J. Phys. B: At., Mol. Opt. Phys. **34**, 1185 (2001).
[26] J. T. Gudmundsson, "Electron excitation rate coefficients for the nitrogen discharge," Report RH=09-2005, Science Institute, University of Iceland, 2005.
[27] P. C. Cosby, J. Chem. Phys. **98**, 9544 (1993).
[28] J. P. Boris and D. L. Book, J. Comput. Phys. **11**, 39 (1973).
[29] J. Li, W. Sun, B. Pashaie, and S. K. Dhali, IEEE Trans. Plasma Sci. **23**, 672 (1995).
[30] V. F. Tarashenko, G. V. Naidis, D. V. Beloplotov, D. A. Sorokin, M. I. Lomaev, and N. Y. Babaeva, Plasma Phys. Rep. **46**, 320 (2020).
[31] X. Lu, G. V. Naidis, M. Laroussi, S. Reuter, D. B. Graves, and K. Ostrikov, Phys. Rep. **630**, 1 (2016).

© Author(s) 2021